A Deep Novel Study on Different CNN Algorithms for Face Skin Disease Classification based on Clinical Images

[1]*M.Noor Moyeen* *M.Tech*
[2]*M.Noor Rezwana* *Msc BioChemistry*

ABSTRACT Skin problems not only injure physical health but also induce psychological problems, especially for patients whose faces have been damaged or even disgorged. Using smart devices, most of the people are able to obtain convenient clinical images of their face skin condition. On the other hand, the convolution neural networks (CNNs) have achieved near or even better performance than human beings in the imaging field. Therefore, this paper studied different CNN algorithms for face skin disease classification based on the clinical images. First, from Xiangya_Derm, which is, to the best of our knowledge, China's largest clinical image dataset of skin diseases, we established a dataset that contains 2656 face images belonging to six common skin diseases [seborrhoea kurtosis (SK), actinic kurtosis (AK), rosacea (ROS), lupus erythematosus (LE), basal cell carcinoma (BCC), and squamous cell carcinoma (SCC)].We performed studies using five mainstream network algorithms to classify these diseases in the dataset and compared the results. Then, we performed studies using an independent dataset of the same disease types, but from other body parts, to perform transfer learning on our models. Comparing the performances, the models that used transfer learning achieved a higher average precision and recall for almost all structures. In the test dataset, which included 388 facial images, the best model achieved 92.9%, 89.2%, and 84.3% recalls for the LE, BCC, and SK, respectively, and the mean recall and precision reached 77.0% and 70.8%.

INDEX TERMS: Deep learning, CNN, facial skin disease, medical image processing.

1. INTRODUCTION

Based on a survey in 2010, skin diseases had the fourth leading cause of nonfatal disease burden in the world, and three of the world's most common diseases were skin dis-eases [1]. Skin diseases have caused enormous economic burdens both in high-income and low-income countries. For each individual, skin problems can have adverse effects on all aspects of life, including interpersonal relationships, work, social functioning, physical activity and mental health.

Usually, skin diseases cause skin lesions, scales, plaques, pigmentation and other symptoms on the patient's skin [2] [5]. These symptoms result in long-term pain and dis gurement. Such damage not only injures physical health but also contribute to serious mental problems, especially when such damage occurs on face. Studies [6] [8] showed that patients with primary skin diseases (such as psoriasis, alopecia areata and vitiligo) have a higher potential for mental problems, such as anxiety and depression. In addition, some skin disease treatments also have the possibility of inducing mental illness (such as isotretinoin, an acne medication, may induce suicidal depression).

Facial skin is exposed to the air almost all the time, so it has a higher risk of being damaged than other areas. Moreover, facial skin is the most important part of the body for people's appearance, so people are more concerned about their facial skin health than skin health anywhere else.

Along with the availability of massive amounts data brought by the Internet [9] and the improvement of com-puting power brought by advanced hardware, deep learning algorithms have achieved human-level performance in many elds. For example, convolutional neural networks (CNNs) have made many breakthroughs in the eld of medical image processing, especially for pathological, CT and MRI images, which have rigid features and high resolution. However, research on clinical images is relatively insuf cient. For these reasons, clinical images always contain a very complex

con-text, and it is hard to control the conditions of acquiring the image. These circumstances make image processing tasks dif cult.

Furthermore, datasets of a certain part of the body, espe-cially the face, re relatively scarce. At present, most of the available datasets are not clearly labeled with information on the body parts; for some datasets that provide this informa-tion, the proportion of facial images is always small [10]. All of these conditions make research dif cult.

Therefore, this paper rst constructed a skin image dataset based on 6 common facial skin diseases (seborrheic keratosis (SK), actinic keratosis (AK), rosacea (ROS), lupus erythe-matosus (LE), basal cell carcinoma (BCC), and squamous cell carcinoma (SCC)). It includes 2,656 facial images for a total of 4,394 images. We focus on these diseases for the following reasons: 1) LE, ROS, BCC and SCC frequently occur on the face; 2) AK and SK usually transition from benign to malignant without timely treatment.

Based on the dataset, experiments were carried out on 5 different CNN structures to verify whether these methods can effectively diagnose facial skin diseases using clinical images. In the test set consisting entirely of facial images, the structure named Inception-ResNet-v2 achieved the high-est average precision (77.0%).

II. RELATED WORKS

Many studies have applied deep learning algorithms to skin diseases [10] [12]. For example, the performance in the task of classifying skin tumors using the Inception-v3 network has reached the level of professional dermatologists; for nine classes of tumors, a computer achieved an accuracy of 55.4%, and two dermatologists achieved accuracies of 53.3% and 55.0% [10]. Using the same network structure, [11] achieved an accuracy of 87.25 2.24% on the dermoscopic images for four common skin diseases, including SK, BCC, psoria-sis and melanocytic nevus. These studies show that current deep learning methods have the potential to be applied to dermatoses.

At the same time, the application of deep learning to face-related diseases is also promising. Reference [13] designed a deep learning algorithm called DeepGestalt and trained their model on more than 17,000 real facial images of genetic syndromes, and this model can identify more than 200 genetic syndromes using facial images with relatively high precision. Reference [14] investigated using CNNs to classify acne into different severity grades ranging from clear to severe, and their results show that the accuracy of their method outperformed expert physicians.

Initially, we investigated the proportion of facial images in the most commonly used public datasets for skin dis-ease, which include AtlasDerm [15], DermlS [16], the ISIC Archive [17], Derm101 [18] and Dermnet [19]. Most of these datasets [15] [18] did not provide information about body parts. In [19], which does provide body parts infor-mation, there were only 195 facial images. It is dif cult to perform further research on facial skin diseases using such limited data. As a result, building a specialized dataset for face images is extremely necessary for our research.

III. FACE IMAGE DATASET

First, this paper established a dataset based on facial skin disease images, including 6 common skin diseases. The images in the dataset were obtained from Xiangya-Derm. These images and labels were rigorously reviewed by at least three experienced dermatologists. It will be made public after relevant procedures are completed.

Xiangya-Derm consists of 150,223 clinical images from 543 different skin diseases. Each image is captured by digital camera and has a matched pathology and medical history. This construct was produced by the Department of

Dermatol-ogy, Xiangya School of Medicine, Central South University. To the best of our knowledge, it is the largest clinical image dataset of skin disease for computer-aided diagnosis (CADx).

The details of the data distribution are shown in Table 1 and Figure 1. It is worth mentioning that the training set and the test set are divided according to different patients, which means that images of the same patient are prevented from appearing in both the training set and the test set.

Our study was approved by the Ethics Committee of Xiangya School of Medicine, Central South University, and all participants provided informed consent.

IV. METHODS

A neural network is a mathematical model inspired by the transfer process of biological neuron information, and its purpose is to learn a mapping from input to output. By using a loss function as a constraint and backpropagation to optimize the parameters, this method can automatically learn complex tasks for different elds. This method has reduced the need for human labor, such as manual feature extraction and data reconstruction for classi cation. A CNN is a type of neural network. It generally consists of an input layer, many hidden convolutional layers, and an output layer. Using this struc-ture, the model can include a large number of parameters and obtain some usable properties, such as equivariance, for image-related tasks.

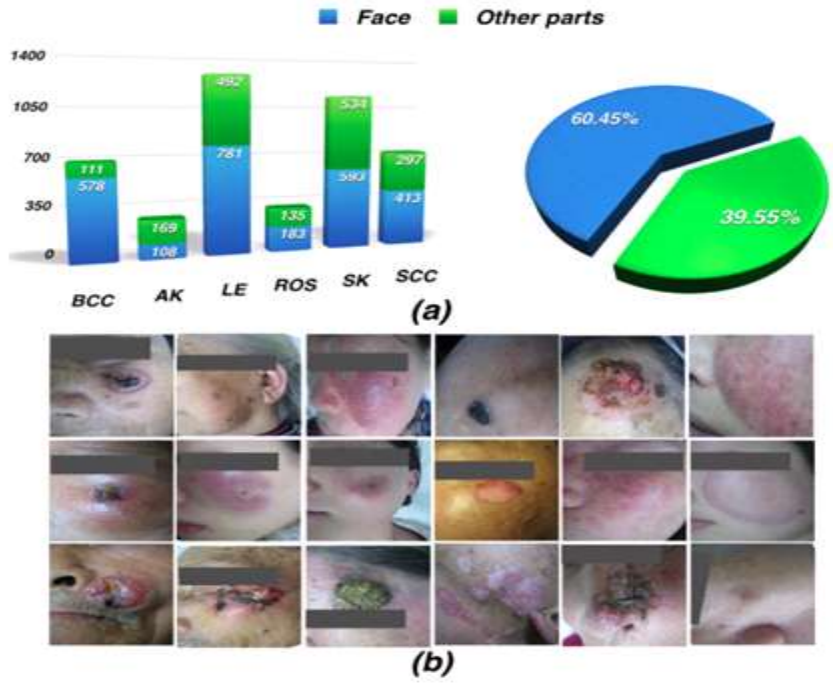

FIGURE 1. The stacked cylinder diagram ((a) left) and the pie chart ((a) right) show the distribution of the images of face and other body parts for different diseases in the dataset; (b) shows some examples of the dataset.

TABLE 1. Summary of dataset.

	IMAGE QTY	Face image		
BCC	689	578	623	66
AK	277	108	219	58
LE	1273	781	1188	85
ROS	318	183	263	55
SK	1127	593	1075	52
SCC	710	413	638	72
Total	4394	2656	4006	388

In this paper, we used ve mainstream CNN algorithms that have been pretrained on ImageNet [9]. These ve structures include ResNet-50, Inception-v3, DenseNet121, Xcep-tion and Inception-ResNet-v2. We used same pre-process for these images, including random reverse and crop. And to address the problem of data imbalance, we used different weights in the cost function for different diseases.

ResNet adds connections between the shallow and deep layers of the network. Such connections directly transmit the information of the shallow layer to the deep layer. On the other hand, the propagation of the gradient to the shallow layer during backpropagation greatly increases the number of network layers [20].

The basic module of the Inception structure is the inception block. There are different kernels in a block, and each type of kernel has a different shape; the output of the block is combines the output from different kernels. This improves the diversity of the network in terms of width and the diver-sity of the scale of the receptive eld. Therefore, the model improved its recognition performance for objects with differ-ent sizes [21], [22].

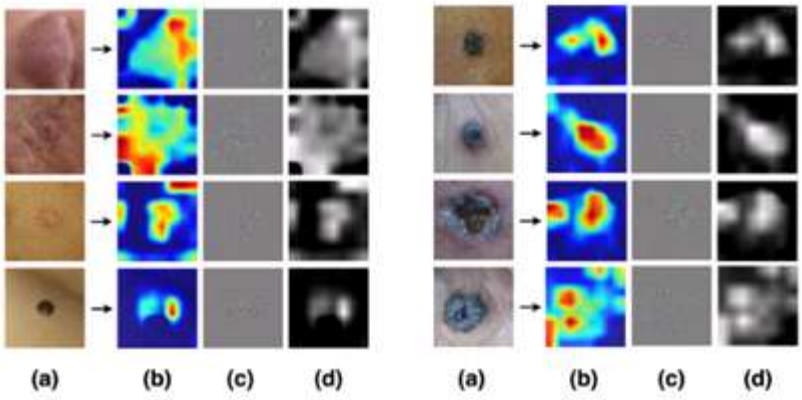

FIGURE 2. (a) is the input images, (b) is the heatmap for the combination of input images and the corresponding output of grad-CAM(d). (c) is the output of guided propagation.

DenseNet adds connections between each two layers; that is, the output feature maps of each layer will be used as the input for all subsequent layers. Using these dense connec-tions, the network reuses features, thereby improving perfor-mance with fewer parameters, which makes the calculation more ef cient [23].

Xception is an updated version of the Inception structure. Xception improves the Inception module with a depthwise separable convolution. This change decouples spatial correla-tions and cross-channel correlations. It can obtain a better per-formance than Inception-v3 with the same parameters [24].

To some extent, Inception-ResNet is a combination of Inception and ResNet structures. By adding a residual connection to the Inception network, it can train deeper networks while maintaining the scale diversity of the network, thereby enhancing the performance [25].

In this paper, we used the same 300 300 input images for each network and did not change the basic structure from that in their origin paper. We replaced the rst fully connected layer behind the last convolutional layer with global aver-age pooling and a 1 1 convolution to reduce the number of parameters and maintain spatial information. Finally, we used a 1024-d fully connected layer in each network and then used a softmax or logistic regression classi er to obtain 6 con dence outputs for six facial skin diseases. More details about the model structures are shown in Table 2, where *incep-tion block, dense block, transition layer,*and*inception resnet block*are modules that are the same as those from the origin papers.

V. RESULTS AND DISCUSSIONS

First, the ve models are trained using only clinical facial images. The results obtained are shown in Table 3. The Inception-ResNet-v2 structure achieved the highest perfor-mance. Then, we pretrained the model with the data of other body parts and used the parameters from the pretrained model as the initial parameters for the new model, which is a method called transfer learning. The results are shown in Table 4.

Comparing the results of Tables 3 and 4, the performance of the models that were pretrained on other body part images are generally superior to those models that were trained using only the facial images. In our opinion, there are so many differences between the images of different parts of the body.

TABLE 2. Structures of the five models.

ResNet50	Inception V3	*DenseNet-121*		
Input layer 10*10*64, S=2, P=3*3, S=2, Out=75*75*64	**Input layer** 3*3*32, S=2, Out=150*150*32	**Input layer** 10*10*16, S=2, P=3*3, S=2, Out=75*75*16	**Input layer** 3*3*32, S=2, 3*3*64, Out=150*150*64	**Input layer** **(Stem)** 3*3*32, S=1, 3*3*32, 3*3*64, Out=147*147*64
Conv1.x [1*1*64, 3*3*64, 1*1*256]*3 Out=75*75*256	**Conv1.x** 3*3*32, S=1, 3*3*64, S=1, P=3*3, S=2, Out=75*75*64	**Dense_block1** [1*1, 3*3]*6 Out=38*38*160 **Transition layer1** 1*1, P=2*2, S=2, Out=38*38*160	**Entry flow** [3*3, 3*3, P=3*3, S=2] *3 Concat each block by 1*1 Conv and S=2 Out=19*19*728	**Mix** Mixed_3a Out=73*73*160 Mixed_4b Out=71*71*192 Mixed_5a Out=35*35*384
Conv2.x [1*1*128, 3*3*128, 1*1*512]*4 Out=38*38*512	**Conv2.x** 3*3*80, S=1, 3*3*192, S=2, 3*3*288, S=1, Out=38*38**288	**Dense-block2** [1*1, 3*3]*12 Out=38*38*304 **Transition layer2** 1*1, P=2*2, S=2, Out=19*19*304	**Middle Flow** [3*3*728] *3 *8	Out=35*35*256 **Reduction-A** Out=17*17*896
Conv3.x [1*1*256, 3*3*256, 1*1*1024] *6 Out=19*19*1024	**3 * inception block** Out=19*19*768 **5 * inception block** Out=10*10*1280	**Dense-block3** [1*1, 3*3]*24 Out=19*19*448 **Transition layer3** [1*1, 3*3]*12 Out=10*10*448	**Exit flow** 3*3*728, *3*1024, P=3*3, S=2, 3*3*1536, 3*3*2048, Out=10*10*2048	Out=17*17*896 **Reduction-B** Out=8*8*1792
Conv4.x [1*1*512, 3*3*512, 1*1*2048] *3 Out=10*10*2048	**2 * inception block** Out=10*10*2048	**Dense-block4** [1*1, 3*3]*16 Out=10*10*595	**Global Average Pool** Out=1*1*2048	Out=8*8*1792
Global Average Pool Out=1*1*2048 **Fully Connected** Out=1024 **Softmax** Out=6	**Global Average Pool** Out=1*1*2048 **Fully Connected** Out=1024 **Softmax** Out=6	**Global Average Pool** Out=1*1*1507 **Fully Connected** Out=1024 **Softmax** Out=6	**Fully Connected** Out=1024 Out=6	**Global Average Pool** Out=1*1*1792 **Fully Connected** Out=1024 **Softmax** Out=6

TABLE 3. Results of the model which have not been pre-trained by images of other body parts.

Net		*BCC*	*LE*	*ROS*	*SK*	*AK*	*SCC*	*Average*
Resnet50	*Recall (%)*	*61.5*	*96.4*	*37.8*	*76.5*	*40.0*	*47.9*	**56.7**
	Precision (%)	*47.6*	*56.2*	*64.1*	*70.9*	*40.0*	*55.7*	**55.8**
Incpetion V3	*Recall (%)*	*63.1*	*95.2*	*37.0*	*76.5*	*46.7*	*51.0*	**59.9**
	Precision (%)	*39.4*	*62.0*	*55.3*	*61.9*	*43.8*	*66.7*	**54.9**
Densenet-121	*Recall (%)*	*70.8*	*92.9*	*37.0*	*76.5*	*66.7*	*55.1*	**64.8**
	Precision (%)	*52.9*	*54.9*	*50.9*	*78.0*	*57.1*	*57.1*	**58.5**
Xception	*Recall (%)*	*52.9*	*94.9*	*40.5*	*78.0*	*57.1*	*57.1*	**63.4**
								61.8
Inception-Resnet V2								**67.2**
								63.7

However, for most diseases, the difference in symptoms on different body parts is not obvious. Therefore, when training the model for skin diseases, a better strategy would be to use the data of the whole body to train the model and then use it as the initialization and retrain model on images of a particular body part. Then, the model can be used to diagnose the disease at that speci c body part.

As shown in Table 3 and Table 4, among the ve network structures, the Inception-ResNet-v2 structure achieved a bet-ter performance. However, the recall for AK is only 54.1%.

TABLE 4. Results of the model which has been pre-trained by images of other body parts.

Net		BCC	LE	ROS	SK	AK	SCC	Average
Resnet50	Recall (%)	74.2	78.6	53.3	76.3	42.7	55.3	63.4
	Precision (%)	60.4	59.5	94.7	53.0	48.5	61.5	62.9
Incpetion V3	Recall (%)	79.2	87.6	62.6	64.5	47.6	58.2	66.6
	Precision (%)	45.5	62.1	92.9	74.5	53.3	55.6	64.0
Densenet-121	Recall (%)	76.9	84.8	58.2	76.5	47.6	65.2	68.2
	Precision (%)	57.5	60.1	93.6	61.9	62.4	77.1	68.8
Xception	Recall (%)	83.1	87.8	58.1	82.2	50.3	62.1	70.6
								68.1
Inception-Resnet V2								77.0
								70.8

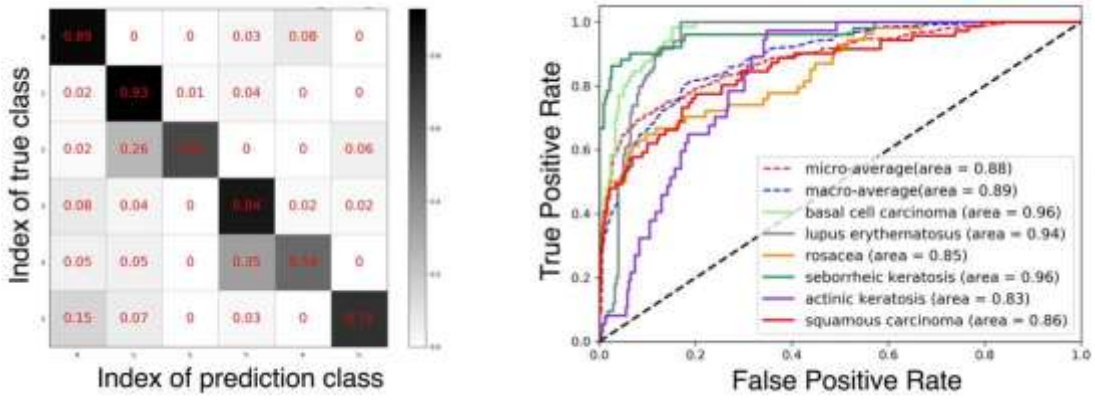

FIGURE 3. Confusion matrix (left) and ROC curve (right) of the Inception-ResNet v2 model on the test set. Class 0-5 are corresponding to BCC, LE, ROS, SK, AK, SCC respectively.

By analyzing the confusion matrix (Figure 3), we found that most of the misjudgment samples of AK were classi ed as SK. After consulting experts, we believe that the primary rea-son is the similar clinical manifestations between SK and AK, which include brown rashes, at papules and local keratoses.

Another possible reason is the imbalance in the number of samples for these two diseases. In the dataset, the number of SK images is signi cantly more than the number of AK images. These two reasons combined cause misclassi

ca-tions. As a result, we believe that at such an insuf cient data scale, it is hard for current CNN structures to determine the difference between such similar diseases. This issue should be studied in future studies.

Furthermore, a drawback of deep learning is that the out-put is hard to explain. To explore what the networks have learned from these images indeed, we used grad-CAM [26] and guided propagation [27] to visualize the output results of Inception-ResNet-v2. For a particular output class, areas that contribute more to classi cation than other areas are shown in warmer colors in the heatmap. The results [Figure 2] show that, generally, CNNs indeed made their predictions by using features learned from lesion areas or other areas with abnormalities, rather than from the textures or other features of normal skin.

VI. CONCLUSION

This paper performed experiments using ve mainstream CNN structures for the clinical image diagnosis of six common facial skin diseases and constructed a data set consisting mainly of facial skin disease images. The results demonstrate that CNNs have the ability to recognize facial skin diseases. Based on our experiments, we determined that different models to diagnose diseases on different body parts should be used. Furthermore, our experiments also showed that a more reasonable network structure could improve the performance of the model. The performance of the current network structure has been satisfactory in some diseases, but the overall performance has yet to be improved. As a result, if we want that people to actually use this technique to check their face skin health in their daily life, specialized improvements should be developed.

In our opinion, the application of arti cial intelligence techniques in the medical eld is not suf cient, and the datasets from this eld should be improved both in quantity and quality. With the increasing amount of facial image data of various skin diseases and the continuous improvement of the network structure, CNN-based facial skin disease diagnosis algorithms will continue to improve in performance. We believe that, in the future, patients will use convenient CNN-based applications to keep their face skin healthy.

REFERENCES

1. R. J. Hay, N. E. Johns, H. C. Williams, I. W. Bolliger, R. P. Dellavalle, and J. Margolis, ‘‘The global burden of skin disease in 2010: An analysis of the prevalence and impact of skin conditions,’’ J. Investigative Dermatol-ogy, vol. 134, no. 6, pp. 1527 1534, 2014.
2. X. Huang, J. Zhang, J. Li, S. Zhao, Y. Xiao, Y. Huang, D. Jing, L. Chen, Zhang, J. Su, Y. Kuang, W. Zhu, M. Chen, X. Chen, and M. Shen, ‘‘Daily intake of soft drinks and moderate-to-severe acne vulgaris in Chinese Adolescents,’’ J. Pediatrics, vol. 204, pp. 256 262, Jan. 2018.
3. Y. Deng, Q. Peng, S. Yang, D. Jian, B. Wang, Y. Huang, H. Xie, and J. Li, ‘‘The rosacea-speci c quality-of-life instrument (RosQol): Revision and validation among Chinese patients,’’ PLoS ONE, vol. 13, no. 2, Feb. 2018, Art. no. e0192487.
4. C. Junchen, W. Zeng, W. Pan, C. Peng, J. Zhang, J. Su, W. Long, Zhao, X. Zuo, X. Xie, J. Wu, L. Nie, H.-Y. Zhao, H.-J. Wei, and Chen, ‘‘Symptoms of systemic lupus erythematosus are diagnosed in leptin transgenic pigs,’’ PLoS Biol., vol. 16, no. 8, Aug. 2018, Art. no. e2005354.
5. X. Xiaoyun, H. Chaofei, Z. Weiqi, C. Chen, L. Lixia, L. Queping, P. Cong, Shuang, S. Juan, and C. Xiang, ‘‘Possible involvement of F1F0-ATP synthase and intracellular ATP in Keratinocyte differentiation in normal skin and skin lesions,’’ Sci. Rep., vol. 7, Feb. 2017, Art. no. 42672.
6. Bewley, ‘‘The neglected psychological aspects of skin disease,’’ Brit. Med. J., vol. 358, p. 3208, Jul. 2017.

7. W. Chen, X. Zhang, W. Zhang, C. Peng, W. Zhu, and X. Chen, ‘‘Polymor-phisms of SLCO1B1 rs4149056 and SLC22A1 rs2282143 are associated with responsiveness to acitretin in psoriasis patients,’’ Sci. Rep.. vol. 4, no. 1, 2018, Art. no. 13182. doi: 10.1038/s41598-018-31352-2.
8. X. Zhou, W. Zhu, M. Shen, Y. He, C. Peng, Y. Kuang, J. Su, S. Zhao, Chen, and W. Chen, ‘‘Frizzled-related proteins 4 (SFRP4) rs1802073G allele predicts the elevated serum lipid levels during acitretin treatment in psoriatic patients from Hunan, China,’’ PeerJ, vol. 13, no. 6, 2018, Art. no. e4637.
9. J. Deng, W. Dong, R. Socher, L. J. Li, K. Li, and L. F. Fei, ‘‘ImageNet: A large-scale hierarchical image database,’’ in Proc. IEEE Conf. Comput. Vis. Pattern Recognit., Jun. 2009, pp. 248 255.
10. Esteva, B. Kuprel, R. A. Novoa, J. Ko, S. M. Swetter, H. M. Blau, and Thrun, ‘‘Dermatologist-level classi cation of skin cancer with deep neural networks,’’ Nature, vol. 542, pp. 115 118, Feb. 2017.
11. X. Zhang, S. Wang, J. Liu, and C. Tao, ‘‘Towards improving diagnosis of skin diseases by combining deep neural network and human knowledge,’’ Med. Inform. Decis. Making, vol. 18, no. 2, p. 59, 2018.
12. Masood and A. A. Al-Jumaily, ‘‘Computer aided diagnostic support system for skin cancer: A review of techniques and algorithms,’’ Int. Biomed. Imag., vol. 2013, pp. 1 22, 2013.
13. Y. Gurovich, Y. Hanani, O. Bar, G. Nadav, N. Fleischer, D. Gelbman, Basel-Salmon, P. M. Krawitz, S. B. Kamphausen, M. Zenker, L. M. Bird, and K. W. Gripp, ‘‘Identifying facial phenotypes of genetic disorders using deep learning,’’ Nature Med., vol. 25, pp. 60 64, Jan. 2019.
14. Melina, N. N. Dinh, B. Tafuri, G. Schipani, S. Nisticò, C. Cosentino, Amato, D. Thiboutot, and A. Cherubini, ‘‘Arti cial intelligence for the objective evaluation of acne investigator global assessment,’’ J. Drugs Dermatology, vol. 17, no. 9, pp. 1006 1009, 2018.
15. Dermatology. Samuel Freire Da Silva, Delso Bringel Calheiros. [Online]. Available: http://www.atlasdermatologico.com.br
16. DermIS.net. The Dept. of Clinical Social Medicine (Univ. of Heidelberg) and the Dept. of Dermatology (Univ. of Erlangen). Accessed: Apr. 2019. [Online]. Available: http://www.dermis.net
17. ISDIS Treasurer, Angel Cummings, Aadi Kalloo, University DermatologyCenter. Accessed: Apr. 2019. [Online]. Available: https://www.isicarchive.com/#!/topWithHead-er/onlyHeaderTop/gallery
18. Derm101. [Online]. Available: https://www.derm101.com/imagelibrary/? match=IN
19. Dermnet, Thomas Habif. [Online]. Available: http://www.dermnet.com
20. K. He et al., ‘‘Deep residual learning for image recognition,’’ 2015.
21. Szegedy, W. Liu, Y. Jia, P. Sermanet, S. Reed, D. Anguelov, D. Erhan,
22. Vanhoucke, A. Rabinovich, ‘‘Going deeper with convolutions,’’ in Proc. IEEE Conf. Comput. Vis. Pattern Recognit., Jun. 2015, pp. 1 9.
23. Szegedy, V. Vanhoucke, S. Ioffe, J. Shlens, and Z. Wojna, ‘‘Rethinking the inception architecture for computer vision,’’ in Proc. IEEE Conf. Comput. Vis. Pattern Recognit. (CVPR), Jun. 2016, pp. 2818 2826.
24. G. Huang, Z. Liu, L. van der Maaten, and K. Q. Weinberger, ‘‘Densely connected convolutional networks,’’ in Proc. IEEE Conf. Comput. Vis. Pattern Recognit., Jul. 2017, pp. 4700 4708.
25. F. Chollet, ‘‘Xception: Deep learning with depthwise separable convolu-tions,’’ in Proc. IEEE Conf. Comput. Vis. Pattern Recognit., Jul. 2016, pp. 1251 1258.

26. Szegedy, S. Ioffe, V. Vanhoucke, and A. A. Alemi, ‘‘Inception-v4, Inception-ResNet and the impact of residual connections on learning,’’ in Proc. 31st AAAI Conf. Artif. Intell., Feb. 2017, pp. 1 7.

27. R. R. Selvaraju, M. Cogswell, A. Das, R. Vedantam, D. Parikh, and

28. Batra, ‘‘Grad-CAM: Visual explanations from deep networks via gradient-based localization,’’ in Proc. IEEE Conf. Comput. Vis. Pattern Recognit., Oct. 2016, pp. 618 626.

29. J. T. Springenberg, A. Dosovitskiy, T. Brox, and M. Riedmiller, ‘‘Striving for simplicity: The all convolutional net,’’ Dec. 2014, arXiv:1412.6806. [Online]. Available: https://arxiv.org/abs/1412.680

AUTHORS

M.Noor Moyeen received his b.tech degree in electronics and communication engineering in 2009 and M.Tech in digital electronics and communication systems in 2013 from Jawaharlal Nehru Technological University, Anantapur, INDIA

M.Noor Rezwana, received her Bsc and Msc in Biochemistry from SrikrishnaDevaraya university Anantapur, INDIA. Currently she is working as a lecturer in S.K.P Governament Degree college, Guntakal, INDIA.